View metadata, citation and similar papers at core.ac.uk

brought to you by CORE

provided by ASU Digital Repository

CMOS On-Chip 3D Inductor Design & Application in RF Bio-Sensing

by

Hemanshu Abbey

A Thesis Presented in Partial Fulfillment
of the Requirements for the Degree
Master of Science

Approved April 2012 by the
Graduate Supervisory Committee:

Bertan Bakkaloglu, Chair
Sayfe Kiaei
Michael Goryll

ARIZONA STATE UNIVERSITY

May 2012

ABSTRACT

Three-dimensional (3D) inductors with square, hexagonal and octagonal geometries have been designed and simulated in ANSYS HFSS. The inductors have been designed on Silicon substrate with through-hole via with different width, spacing and thickness. Spice modeling has been done in Agilent ADS and comparison has been made with results of custom excel based calculator and HFSS simulation results. Single ended quality factor was measured as 12.97 and differential ended quality factor was measured as 15.96 at a maximum operational frequency of 3.65GHz. The single ended and differential inductance was measured as 2.98nH and 2.88nH respectively at this frequency. Based on results a symmetric octagonal inductor design has been recommended to be used for application in RF biosensing. A system design has been proposed based on use of this inductor and principle of inductive sensing using magnetic labeling.

Dedicated to my family and friends

ACKNOWLEDGMENTS

It has been a great honor and privilege to complete my Masters of Science Degree in Electrical Engineering (MSEE) at Arizona State University (ASU).

First of all, I would like to thank my professors Dr. Bertan Bakkaloglu, Dr. Sayfe Kiaei and Dr. Michael Goryll who have provided me with quality instruction, guidance, and motivation to complete this project. They have been a significant source of education and encouragement throughout my graduate college. I would also like to thank them for thoroughly reviewing the research work and thesis.

I also thank Dr. Ali Meaamar who has provided me with countless hours of quality instruction and technical guidance. It was a great learning experience working with him on other project assignments like PLL system level simulation, PFD design and layout and CML buffer layout and simulations.

Finally I would like to thank all my friends and my family for their unfettered support throughout my course-work at Arizona State University.

TABLE OF CONTENTS

Page

CHAPTER Page

LIST OF TABLES

LIST OF FIGURES

Figure Page

CHAPTER 1

INTRODUCTION

Recently, there has been a boom in biomedical application field and an important need for bio-devices has been felt that can quickly and accurately analyze biological samples like bio molecules, DNA or cells. Researchers from many areas of science and engineering are developing a variety of biosensors, aimed at increased sensitivity, portability, power efficiency and low-cost diagnostics. To meet these criterions we need to move towards higher level of integration which commands working with on-chip passives, especially on-chip inductors.

1.1. Motivation for Biosensors

Biosensor can essentially serve as low-cost and highly efficient devices for quickly, reliably, and accurately detecting contaminating bio-agents in the atmosphere in addition to being used in other day-to-day applications. There are several applications of biosensors in food analysis e.g. detecting pathogens and food toxins. Biosensors are being developed for different applications, including environmental and bioprocess control, quality control of food, agriculture, military, and, particularly, medical applications like drug discovery or drug test.

1.2. Motivation for Magnetic Based Inductive Sensing

Future biosensors based on molecular level detection require sensing mechanism which has good sensitivity, portability, power efficiency and has low cost. Magnetic particle based sensing schemes is a promising approach which fulfills the above requirements. Other widely used detection schemes like fluorescence based sensing suffer from heavy cost and setup issues. The

magnetic particle based inductive sensing scheme is based on the fact that an AC electrical current through the on-chip inductor generates a magnetic field and polarizes the magnetic particles present in its vicinity. This increases the total stored magnetic energy in the space and thereby the effective inductance of the inductor. The oscillation frequency of $f_0=1/(2\pi\sqrt{L_0C_0})$, then down-shifts due to the increase in inductance. Thus by measuring the frequency drift we can estimate the number of target particles which were immobilized by magnetic particles.

1.3. Motivation for On-Chip Inductors

Earlier the wide-spread use of inductors in silicon based CMOS circuits was limited by its relatively large size, performance and integration limitations. But now the rapidly growing wireless & RF application industry has driven RFICs to higher level of integration and portability. To achieve this along with meeting requirements like low cost, low power, low noise, low distortion and high frequency operation has been the real challenge. The performance of RF integrated circuits is dependent on the availability of high Q integrated inductors.

Typical Applications of on chip inductors are in integrated RF circuit which involve

- LC tank circuits for low phase noise VCOs
- Input and output matching networks for amplifiers
- Low Noise Amplifiers
- Balun and transformers
- Inductive loaded amplifiers
- Inductive based Biosensors

1.4. Thesis Organization

This thesis aims to provide an insight into design of on-chip inductors and their application in bio-sensor design.

Chapter 2 covers the introduction to Biosensors and their performance metric. It talks about the classification of biosensors and tradeoffs of using labeled vs label free biosensors.

Chapter 3 will propose an approach based on magnetic particle based sensing scheme to design an RF biosensor with application in the field of drug discovery and drug testing. The biosensor system will consist of a voltage controlled oscillator (VCO) and a through-hole symmetric octagonal inductor as a part of LC tank of the VCO. The chapter will also highlight the experiment steps to be performed and the complete proposed system design.

Chapter 4 reviews inductor physics based upon the monolithic planer spiral topology in a CMOS process. This discussion will cover the physical layout, field distribution and basis for shape selection of an on-chip inductor. Chapter 4 will also provide information on non-uniform current distribution effects. It will discuss resistive, capacitive and substrate losses incurred in the on-chip topology. Skin effect and proximity effects observed at high frequencies will also be discussed in detail. Going ahead an introduction to design guidelines for on-chip inductors would be given. These were observed after extensive study of previous research work and conducting HFSS experiments on several designs. The chapter will end by exploring different layout techniques to improve Quality factor.

Chapter 5 will briefly review the various HFSS designs that were made and simulated as a part of research starting from square to octagonal geometries. The discussion will cover stack-up and measured performance of the inductors in terms of values for inductance, series resistance, capacitance etc. The chapter will also present modeling of spiral inductors in ADS and comparing the results with a custom made Microsoft excel based calculator and HFSS measurements. Moving ahead discussion on requirement for a symmetric shaped inductor will be done and from there more concentration will be given to symmetric octagonal geometry design and simulation. The chapter will conclude by a quick discussion on measurement techniques for on-chip inductors that include test and characterization setup.

Chapter 6 will draw conclusions on device performance and discuss possible future work for continued research on the 3D inductor and its applications.

CHAPTER 2

BIOSENSORS

Biosensors are analytical tools for the analysis of bio-material samples to gain an understanding of their bio-composition, structure and function by converting a biological response into a quantifiable signal.

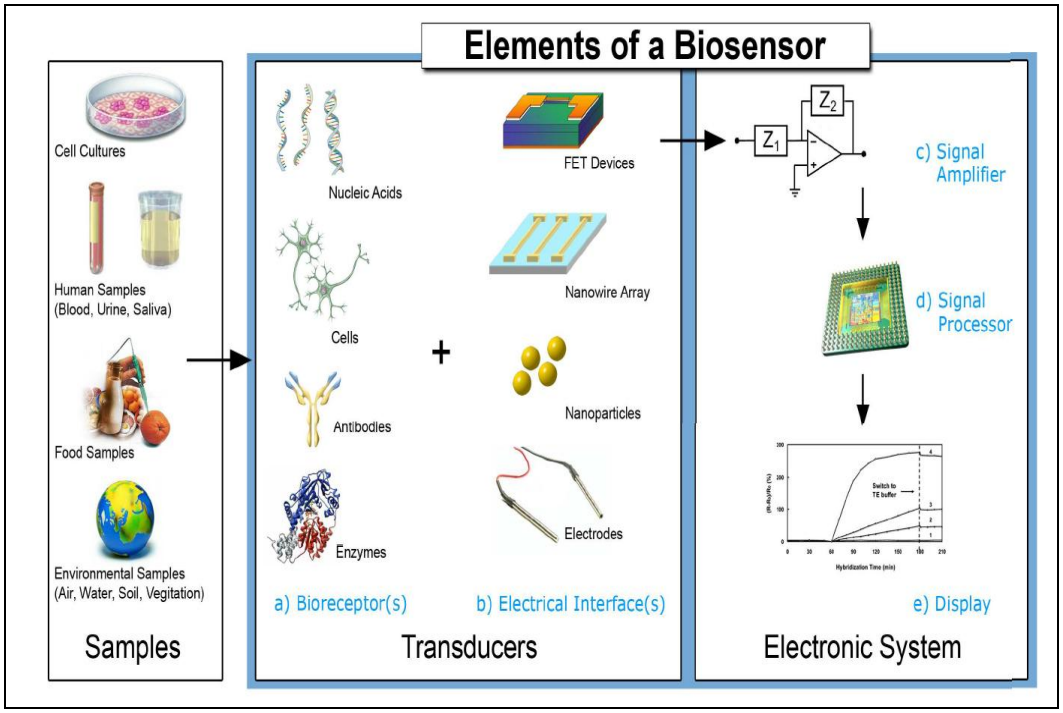

Figure 1: Components of a Biosensor

It consists of 3 parts:

1. A sensitive biological element: It can be a tissue, microorganisms, organelles, cell receptors, enzymes, antibodies or nucleic acids, etc. which interacts (binds or recognizes) the analyte under study. An analyte is a substance that is of interest in an analytical procedure.

2. Transducer: It is the detector element that transforms the signal resulting from the interaction of the analyte with the biological element into another signal that can be more easily measured and quantified.

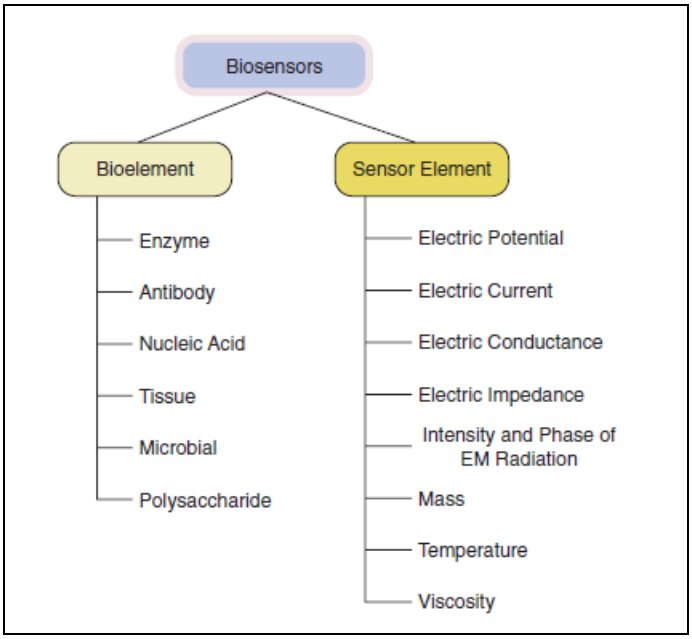

Figure 2: Possible Bio Elements and Sensor Elements

3. Biosensor Reader Device: It is the associated electronics or signal processors that are primarily responsible for the display of the results in a user-friendly way.

Biocatalyst must be highly specific for the purpose of analysis.

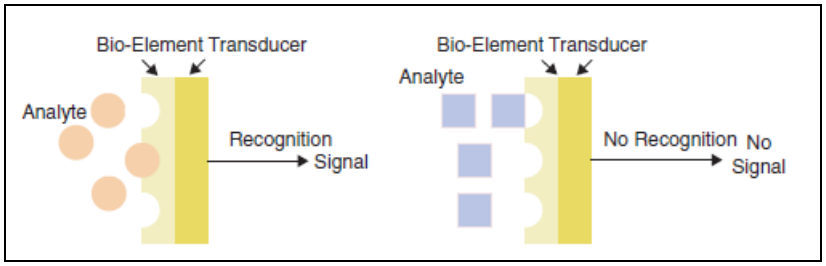

Figure 3: Affinity Based Sensing

2.1. Classification of Biosensors

Biosensors are majorly classified into the following categories:

2.1.1 Electrochemical

Electrochemical biosensors are normally based on enzymatic catalysis of a reaction that produces or consumes electrons (such enzymes are rightly called redox enzymes).They can be further divided into following category.

- Amperometric

An oxidizing potential is applied between the cell electrodes and the cell current which is a result from the oxidation or reduction of an electro-active species in a biochemical reaction is measured. For example the current produced may be directly proportional to the oxygen concentration. The peak value of the current measured over a linear potential range is proportional to the bulk concentration of the analyte. Amperometric based biosensors have better sensitivity compared to the potentiometric devices.

- Potentiometric

In potentiometric biosensors use of ion selective electrodes is done to measure cell potential at zero current by observing the potential difference between reference electrode and potential at the working electrode. Potentiometric biosensors provide the advantage of measuring low concentration in tiny samples since they ideally offer the benefit of not chemically influencing a sample.

- Impedometric

Impedance biosensors measure the electrical impedance of an interface in AC steady state with constant DC bias condition. This is accomplished by imposing a small sinusoidal voltage at a particular frequency and measuring the resulting

current. This process known as Electrochemical Impedance Spectroscopy (EIS) can be repeated at different frequencies. Impedance measurement does not require special reagents and is amenable to label free operation. In impedance biosensors the applied voltage should be quite small usually 10mV amplitude or less. This is because current voltage relationship is often linear only for a small perturbations and high voltage can damage probe-target binding.

2.1.2 Optical

Optical biosensors are a powerful detection and analysis tool and are immune to electromagnetic interference, capable of performing remote sensing and can provide multiplexed detection within a single device. Generally, there are two detection protocols that can be implemented in optical bio-sensing: fluorescence-based detection and label-free detection.

They can be divided in majorly two categories:

- Colorimetric: Measure change in light adsorption
- Photometric: Photon output for a luminescent or fluorescent process can be detected with photomultiplier tubes or photodiode systems.

In fluorescence-based detection, either target molecules or bio recognition molecules are labeled with fluorescent tags, such as dyes; the intensity of the fluorescence indicates the presence of the target molecules and the interaction strength between target and bio-recognition molecules.

2.1.1 Calorimetric

Enzyme catalyzed reactions can be endothermic or exothermic, absorbing or generating heat which can be measured by two thermistors by measuring the difference in resistance between reactant and product and hence the analyte concentration.

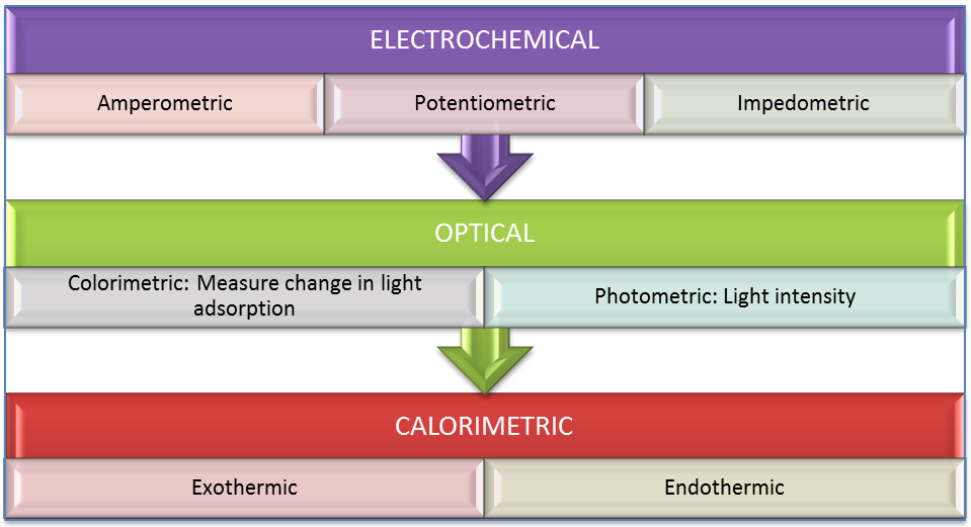

Figure 4: Classification of Biosensors

2.2 Characteristics of Biosensors

1. SELECTIVITY: Sensor detects a certain analyte and does not interact with admixtures and contaminants. For example antigen and antibody interaction has the highest selectivity.

2. SENSITIVITY: Reflects the minimal amount or concentration of analyte that can be detected.

3. PRECISION: It is characterized in terms of standard deviation of measurements.

4. SIGNAL STABILITY: Shows signal drift under constant conditions which causes error in measured concentration. Signal drift is usually measured in percent per hour.

5. RESPONSE TIME: It is defined as the time required to analyze the assay.

6. REGENERATION TIME: It is defined as the time required to return the sensor to working state after interaction with sample.

7. LINEARITY: slope of signal variation vs. concentration of analyte should be constant over a large concentration range.

8. HYSTERESIS: There should be no hysteresis in the system i.e. signal should be independent of prior history of measurements.

9. WORKING RANGE: Range of analyte concentrations in which sensors can operate. Working range of sensor should correlate with the range of possible concentrations of analyte in the assay.

10. COST: The sensor should be of low cost, easy to replace and portable.

2.3. LABELLED vs LABEL FREE BIOSENSORS

Some biosensors require a label attached to the target to enhance the signal discrimination. During readout the amount of label is detected and assumed to correspond to the number of bound targets. Labels can be fluorophores, magnetic beads or active enzymes with an easily detectable product. However, labeling a biomolecule can drastically change the cell properties and have some drawbacks like complicated, time consuming and expensive preparation work.

Label free method that avoids the contamination of the biological media and the influence of the marker on the cell properties. Besides the time and expense benefits of omitting the labeling step, label-free operation enables detection of target-probe binding in real time which is generally not possible with label-based systems. Real-time sensing confers at least two major advantages over endpoint detection. First, time averaging of binding/unbinding events can improve measurement accuracy. Second, it allows determination of affinity constants by curve-fitting the sensor output vs. time

CHAPTER 3

DESIGN PROPOSAL BASED ON INDUCTIVE SENSING

PURPOSE: Sensing of Magnetically labeled target molecules in bioassays

PRINCIPLE: Detecting Frequency Changes in LC Resonant circuit of a cross-coupled VCO

An AC electrical current through the on-chip inductor generates a magnetic field and provides us with a value of inductance. When the bioassay comprising of Enzyme-Linked ImmunoSorbent Assay (ELISA) and magnetic particles used as sensing tags are passed through the core of the inductor, polarization of these magnetic particles takes place. This increases the total stored magnetic energy in the space and hence the effective inductance of the inductor. The oscillation frequency of $f0=1/(2\pi\sqrt{L0C0})$, then down-shifts due to the increase in inductance.

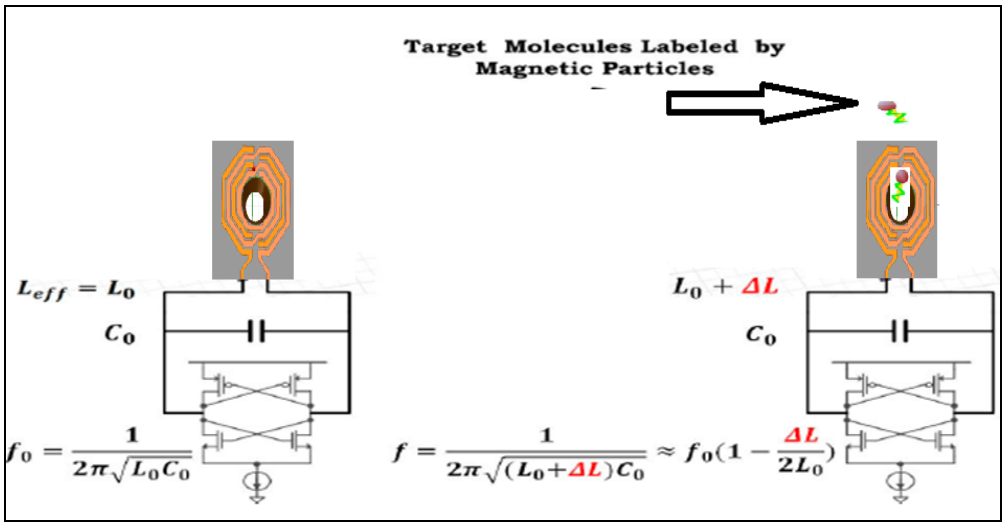

Figure 5: Inductive Sensing

Preparation of Sample:

The pre-deposited molecular probes first capture the target molecules in the sample. The biochemically functionalized magnetic particles are then introduced and immobilized by the captured target molecules. Therefore, by sensing the magnetic particles on the sensor surface, we can directly measure the presence of the target molecules in the test sample.

Note that the frequency shift due to a single micron-size magnetic bead is typically a few parts per million (ppm) of the resonant frequency.

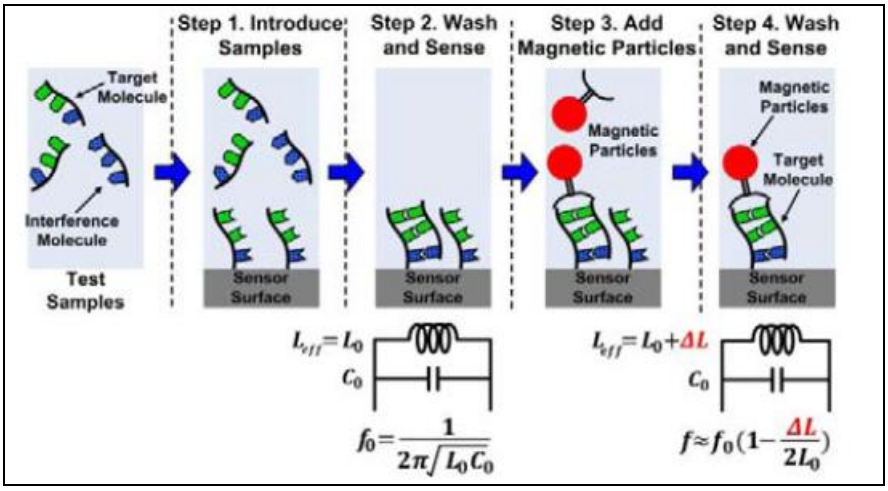

Figure 6: Preparation of Sample for Magnetic Sensing Scheme

Sensor transducer gain defined as the relative frequency-shift (due to the inductance change) per particle is location-dependent and is proportional to the field quantity as well. With our symmetric octagonal Inductor design we can say that the magnetic field distribution at the center of inductor will present a uniform transducer gain.

Experiment Steps:

- Let the bio-sample flow without any magnetic beads and detect the oscillation frequency.
- Now add the biochemically functionalized magnetic particles which then get associated with target molecules. Observe the drift in the resonant frequency.

Design Hurdles Anticipated

- The Frequency Shift due to a single micron size magnetic bead would typically be a few ppm of the resonant frequency. To be able to detect such a small frequency shift we need to down convert the frequency

center cone in KHz range using a step by step down conversion architecture.

- We need to ensure that the VCO design is a low phase noise based.
- Frequency counter design having good counting resolution.
- There is a need to maintain a constant flow of magnetic beads because the resonant shift is dependent on the physical position of the beads.
- Due to magnetic interactions between magnetic beads and the field setup by the inductor there can be a tendency of flow clogging as the magnetic beads can get attracted near to the surface of the inductor.
- Need to suppress any low frequency perturbations like: supply noise, 1/f noise, substrate interference effects, thermal vibrations, low f common mode noise.
- We need to check if there is any possible capacitance change due to presence of magnetic beads.

Bio molecular Sensing Functionality Test

- Need for identification of the bioassays (ELISA) and its electrical properties like permittivity, permeability and loss tangent.
- Design of flow mechanism to allow a constant flow of magnetically labeled target molecules.
- Calibration and interpretation of results. (Frequency Shift variation with Measurement Index, Number of particles in sample, relative distance of individual particles)
- Reproducibility of test results and a comparison of detection efficiency compared to already established old fashion techniques.

- The below through-hole inductor design in proposed. The inductor uses SU-8 as dielectric and for coating the surface to avoid accidental contact by the bioassays.

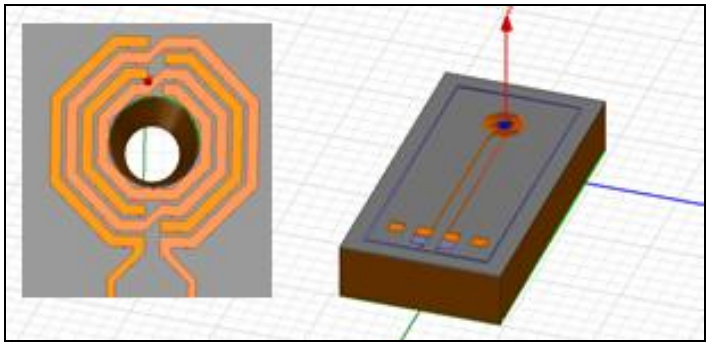

Figure 7: Tapered Through-hole Inductor

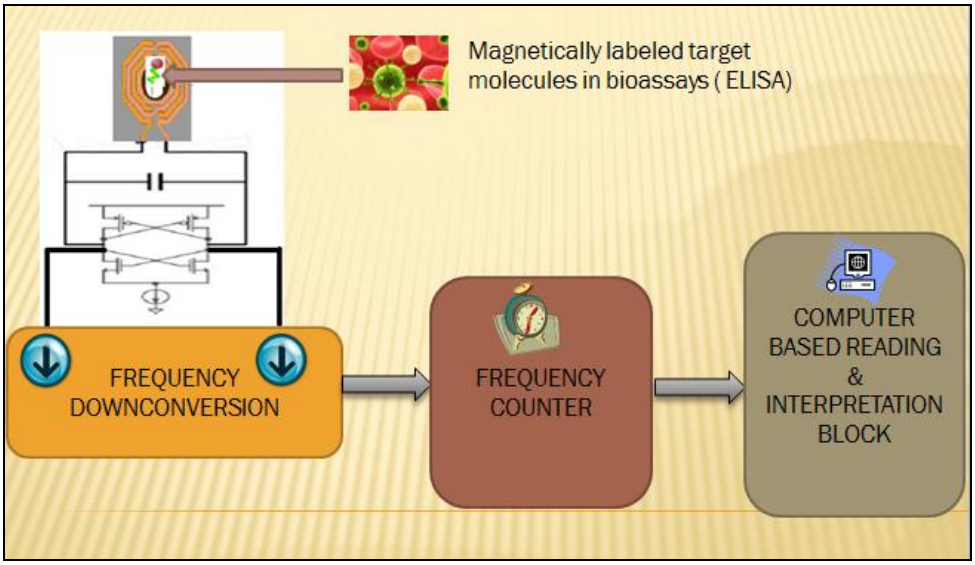

Figure 8: RF-Bio Sensing System Level Flow Diagram

CHAPTER 4

INDUCTOR DESIGN CONSIDERATIONS

Inductance is the ability of an inductor to store energy in a magnetic field. Inductance is really related to the geometry of the conductors. The only thing that influences inductance is the distribution of the conductors and in the case of ferromagnetic metals, their permeability. Inductance is fundamentally related to the number of magnetic-field line loops around a conductor, per amp of current through it. Magnetic-field line loops are always complete circles and always enclose some current.

Some standard definitions

- Inductance: the number of field line loops around a conductor per amp of current through it.
- Self-inductance: the number of field line loops around the conductor per amp of current through the same conductor.
- Mutual inductance: the number of field line loops around a conductor per amp of current through another conductor.
- Loop inductance: the total number of field line loops around the complete current loop per amp of current.
- Loop self-inductance: the total number of field line loops around the complete current loop per amp of current in the same loop.
- Loop mutual inductance: the total number of field line loops around a complete current loop per amp of current in another loop.
- Partial inductance: the number of field line loops around a section of a conductor when no other currents exist anywhere.

- Partial self-inductance: the number of field line loops around a section of a conductor per amp of current in that section when no other currents exist anywhere.
- Partial mutual inductance: the number of field line loops around a section of a conductor per amp of current in another section when no other currents exist anywhere.
- Effective, net, or total inductance: the total number of field line loops around a section of a conductor per amp of current in the entire loop, taking into accounts the presence of field line loops from current in every part of the loop.
- Equivalent inductance: the single self-inductance corresponding to the series or parallel combination of multiple inductors including the effect of their mutual inductance.

4.1. Inductor Physical Layout

Let's discuss the electromagnetic fields generated in planar spiral geometry. When a time varying voltage is applied between the ends of spiral, three electrical and one magnetic field is generated.

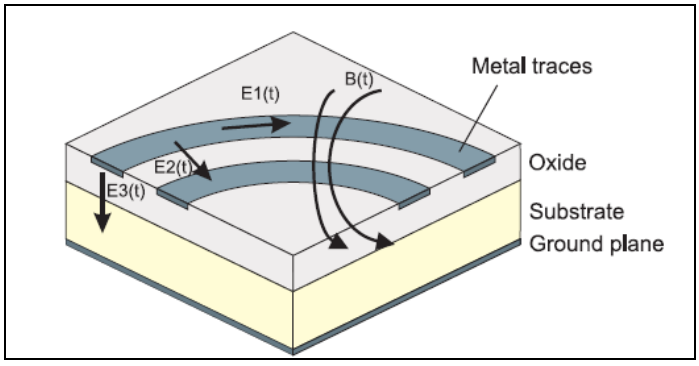

Figure 9: Cross-section of a Planar Inductor

- B(t) responsible for self, mutual and parasitic inductances
- E1(t)is the electric field along the metal trace. It is caused by the current in the winding and the finite conductivity. It is responsible for ohmic losses in the spiral due to resistivity of the metal lines.
- E2(t) Generated as a result of voltage difference between adjacent metal lines and produces capacitive coupling among the coils of the inductor
- E3(t) Generated as a result of existing voltage difference between metal and substrate. It produces capacitive coupling between the spiral and substrate and ohmic losses in substrate due to induced displacement current. In addition to the above electromagnetic fields, many other high-order effects are present.

4.2. Inductor Shape Selection Criteria

- The resistance depends on the perimeter of the loop. Thus, to maximize the Q of the structure, we should utilize a shape with maximum area to perimeter. It is well known that such a shape is indeed a circle. But a rectangular loop has only slightly smaller Q factors and is more convenient for layout.
- Octagonal inductors are preferred over square inductors due to their higher Q factor obtained at a lower inductance and resistance due to a shorter trace length. In other words it’s more area efficient and easier to realize than the circular spiral. They also tend to have lower shunt capacitance

- Research shows that circular shapes result in greater efficiency due to the reduction in current crowding within the device corners. They have the highest Q compared to others but not all processes support fabrication for circular geometry.

For example let's design an inductor with different geometries for a fixed set of parameters as shown below and observe the inductance (in nH) that we get for each of them.

Number of turns (n):	4	turns
Spacing between turns (s):	2	um
Turn width (w):	10	um
Outer Diameter (dout):	192	um
Calculated Inner diameter	100	um
Fill factor p=(Dout-Din)/(Dout+Din)	0.315	

	Square	Hexagonal	Octagonal	Circular
Modified Wheeler	3.68	3.104	3.118	3.137
Current Sheet	3.639	3.158	3.145	3.046
Monomial Fit	3.604	3.153	3.135	3.135

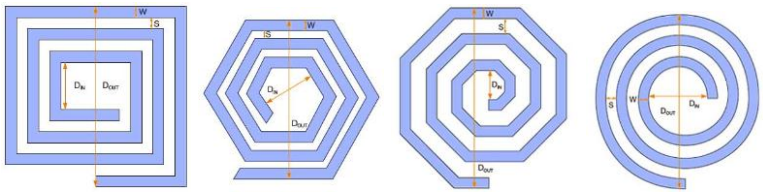

Figure 10: Inductance of Different Geometries

4.3 Non Uniform Current Distribution Effects

When the current distribution is non-uniform, the inductance is no longer current-independent. Eddy current and skin effect result in non-uniform current distribution in the metallic trace of a spiral inductor. We will discuss them in detail along with proximity and ground effects now:

4.3.1 Eddy Current

Eddy current is a current induced on a conductive material through induction from a magnetic field and flow in a circular path. They get their name from “eddies” that are formed when a liquid or gas flows in a circular path around obstacles when conditions are right.

Eddy currents flowing in the material will generate their own “secondary” magnetic field which will oppose the coil’s “primary” magnetic field. Eddy currents are strongest at the surface of the material and decrease in strength below the surface. The depth that the eddy currents are only 37% as strong as they are on the surface is known as the standard depth of penetration or skin depth. This depth changes with probe frequency, material conductivity and permeability.

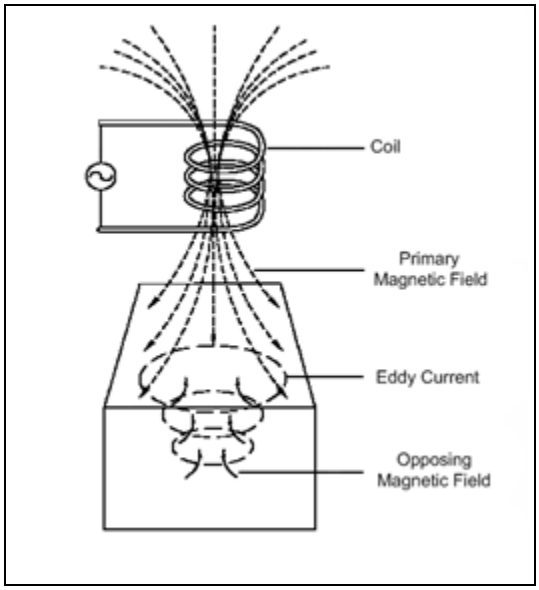

Figure 11: Eddy Currents

Factors affecting the strength of eddy currents:

- Electrical conductivity of the material
- Magnetic permeability of the material

- Amount of solid material in the vicinity of the test coil.

Self-induced eddy currents are responsible for the skin effect in conductors. The latter can be used for non-destructive testing of materials for geometry features, like micro-cracks. A similar effect is the proximity effect, which is caused by externally-induced eddy currents.

Eddy currents are created when a conductor experiences changes in the magnetic field. If either the conductor is moving through a steady magnetic field, or the magnetic field is changing around a stationary conductor, eddy currents will occur in the conductor. The swirling current set up in the conductor is due to electrons experiencing a Lorentz force that is perpendicular to their motion. Hence, they veer to their right, or left, depending on the direction of the applied field and whether the strength of the field is increasing or declining. The resistivity of the conductor acts to damp the amplitude of the eddy currents, as well as straighten their paths. Eddy currents generate resistive losses that transform some forms of energy, such as kinetic energy, into heat. Eddy currents are minimized in these devices by selecting magnetic core materials that have low electrical conductivity.

4.3.2 Skin Effect

Skin effect is the tendency of an alternating electric current (AC) to distribute itself within a conductor with the current density being largest near the surface of the conductor, decreasing at greater depths. In other words, the electric current flows mainly at the "skin" of the conductor, at an average depth called the skin depth. That decline in current density is known as the skin effect and the skin

depth is a measure of the depth at which the current density falls to 1/e of its value near the surface.

The skin effect causes the effective resistance of the conductor to increase at higher frequencies where the skin depth is smaller, thus reducing the effective cross-section of the conductor. The skin effect is due to opposing eddy currents induced by the changing magnetic field resulting from the alternating current.

If current density is represented by J, then:

$$J = J_S e^{-d/\delta} \qquad \delta = \sqrt{\frac{2\rho}{\omega\mu}}$$

δ is called the *skin depth*.

J = constant for uniform current density

J = Jo*$e^{-d/sd}$ for skin effect currents

$$\text{Skin Depth} = \frac{2.602}{\sqrt{f}} \quad \text{inches}$$

In a good conductor, skin depth varies as the inverse square root of the conductivity. This means that better conductors have a reduced skin depth. Skin depth also varies as the inverse square root of the permeability of the conductor. Skin depth is inversely proportional to the square root of the frequency. The frequency where the skin effect just starts to limit the effective cross sectional area of the conductor is called the crossover frequency

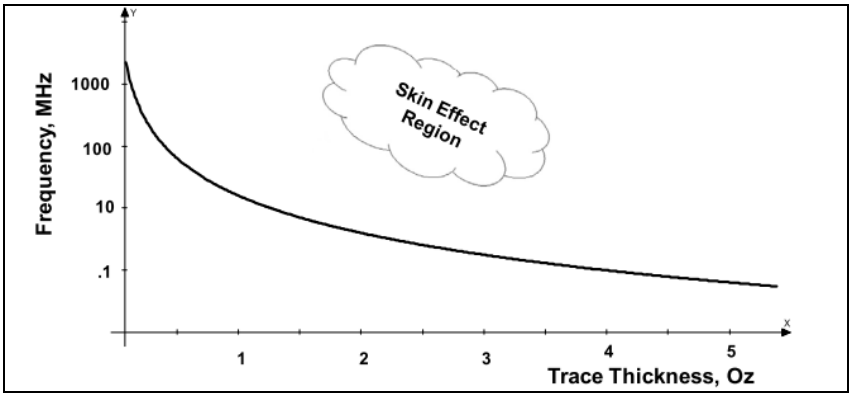

Figure 12: Skin Effect

Skin depth does not depend on the shape of the conductor. Skin depth is a distance measured in from the surface of the conductor toward the center of the conductor. If skin depth is deeper than the center of the conductor, the current is not limited by the skin effect and the current is flowing uniformly throughout the entire cross sectional area of the conductor. Therefore, a thicker conductor is limited by the skin effect at a lower frequency than is a thinner conductor.

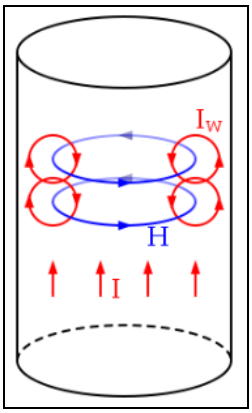

Figure 13: Cancellation of Electric Fields

Skin depth is due to the circulating eddy currents (arising from a changing H field) cancelling the current flow in the center of a conductor and reinforcing it in the skin.

Some important points to consider before we proceed:

- The resistance of a conductor is inversely proportional to the cross sectional area of the conductor. If the cross sectional area decreases, the resistance goes up. The skin effect causes the effective cross sectional area to decrease. Therefore, the skin effect causes the effective resistance of the conductor to increase.
- The skin effect is a function of frequency. Therefore, the skin effect causes the resistance of a conductor to become a function of frequency

(instead of being constant for all frequencies.) This, in turn, impacts the impedance of the conductor. If we are concerned about controlled impedance traces and transmission line considerations, the skin effect causes trace termination techniques to become much more complicated.

- If the skin effect causes the effective cross sectional area of a trace to decrease and its resistance to increase, then the trace will heat faster and to a higher temperature at higher frequencies for the same level of current.

4.3.3 Proximity & Ground Effects

When a signal is close to its return, a mutual inductance exists which may further distort the current flow. Consider a rectangular trace routed directly over and close to a reference plane. If the frequency harmonics are high enough, the skin effect results in the current flowing through an effective cross sectional area that is a rectangular shell around the edges of the conductor. At the same time, the mutual inductance between the signal current (on the trace) and its return (on the plane) causes the return current to locate itself as close as possible to the signal --- i.e. on the plane directly under the trace. This same effect causes the signal current in the rectangular shell to locate more on the planar side of the shell than on the outer side of the shell. This effect is called the “ground effect”

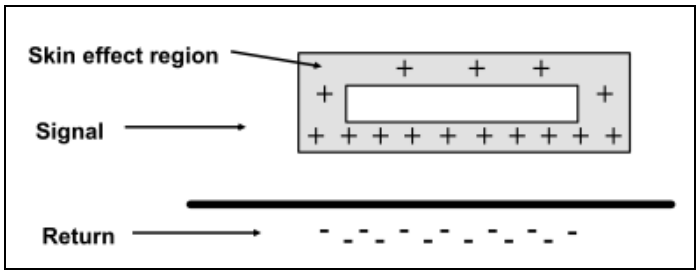

Figure 14: Proximity Effect

A similar effect occurs when a signal and its return are on closely spaced wires or traces as is the case with differential signals. The mutual inductance between the two traces causes the signal currents to distort to the side of the effective cross sectional area between the two traces. This is termed the “proximity effect.” Because the returning signal current at high-frequencies flows in a finite area of the reference plane the effective resistance of the reference plane must be non-zero. The total resistive circuit losses due to the high-frequency pattern of current flow in the reference plane totals approximately 30 percent of the PCB skin-effect trace resistance, a percentage that remains fixed as a function of frequency.

Since the proximity and ground effects distort the current path of the signals through the conductors, they further distort the effective cross sectional area of the conductor, further increasing the effective resistance of the conductor. These effects are very difficult to quantify.

The proximity effect does play a role in determining the patterns of current flow (and therefore the attenuation and characteristic impedance) of micro-strip and strip-line transmission lines. At low frequencies current in a PCB follows the path of least resistance. The path of least resistance for current flowing in a PCB trace fills the volume of the trace, flowing uniformly throughout the conductor. The path of least resistance for that same current as it returns to its source through the power and/or ground planes spreads out in a wide, flat sheet, tending to occupy as much of the surface area of the planes as possible on its way back to the source.

Above a few Megahertz, the magnetic forces become VERY significant, and the current flow patterns change. Above a few Megahertz the inductance of the

traces and planes becomes vastly more important than their resistance, and current flows in the least inductance pathway.

Due to proximity and skin effects metal resistance increases and inductance decreases with the increase in frequency.

We can state the general principle of least-inductive current flow in a number of equivalent ways:

- Current at high frequencies distributes itself to neutralize all internal magnetic forces, which would otherwise shift the patterns of current flow.
- In more technical terms, the component of the magnetic field normal to a (good) conductor is (nearly) zero. (If the normal component is non-zero, eddy currents build up within the conductor to neutralize the normal component of the field).
- In terms of minimum-potential energy, current at high frequencies distributes itself in that pattern which minimizes the total stored magnetic field energy.
- In terms of inductance, current at high frequencies distributes itself in that pattern which minimizes the total inductance of the loop formed by the outgoing and returning current.
- The current in two round, parallel wires is not distributed uniformly around the conductors. The magnetic fields from each wire affect the current flow in the other, resulting in a slightly non-uniform current distribution, which in turn increases the apparent resistance of the conductors. In parallel round wires we call this the proximity effect.

4.3.4 Loss Mechanism in Spiral Inductors

An inductor's loss depends on the geometry of the inductor, metal conductivity, substrate resistivity, and frequency of operation. Metal losses dominate at low frequencies, whereas substrate losses are critical at high frequencies

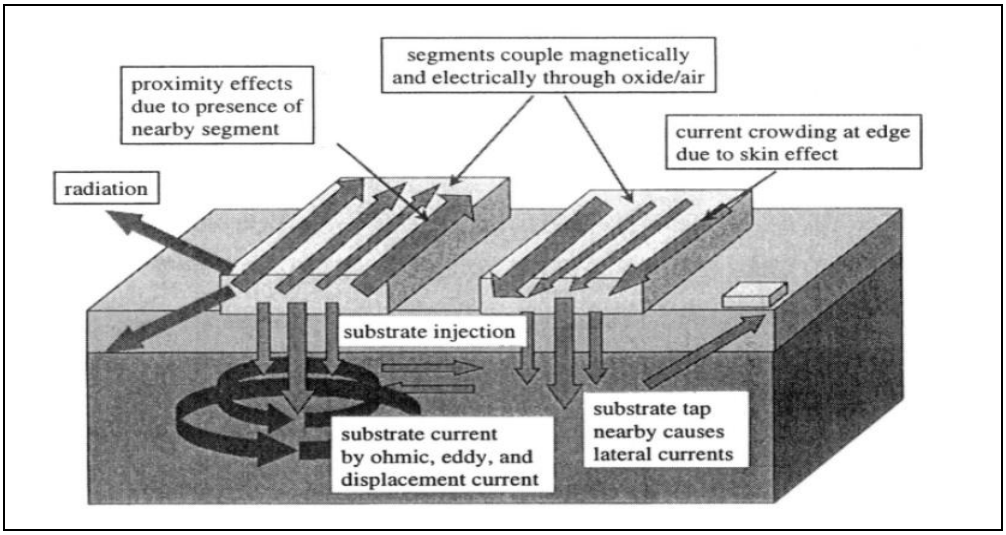

Figure 15: Losses in Silicon Spiral Inductors

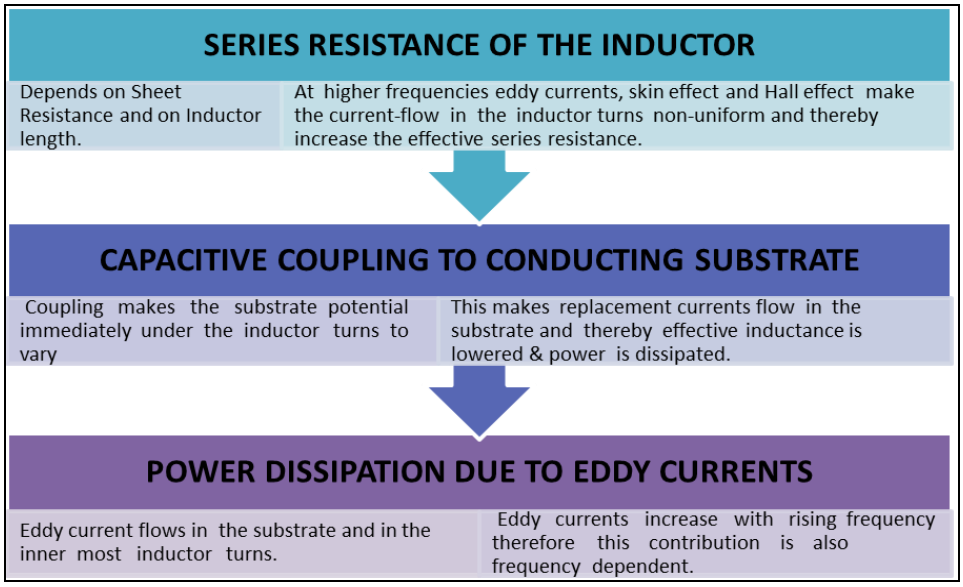

Figure 16: Classification of Losses in Spiral Inductor Design

4.3.5 Substrate Loss

These losses primarily caused by the eddy current, which is induced by magnetic coupling to the substrate. The eddy current flows in silicon substrate with a low resistivity of 8Ω-cm.

Capacitive Losses: Finite resistance due to electrically induced conductive & displacement currents

Magnetic Losses: Magnetically induced eddy current resistance

Due to the Faraday-Lenz law, loops of eddy currents Isub flow in the low-resistivity substrate underneath the coil, with higher current density closer to the coil. The direction of Isub is opposite to the direction of Icoil , giving rise to extra substrate loss.

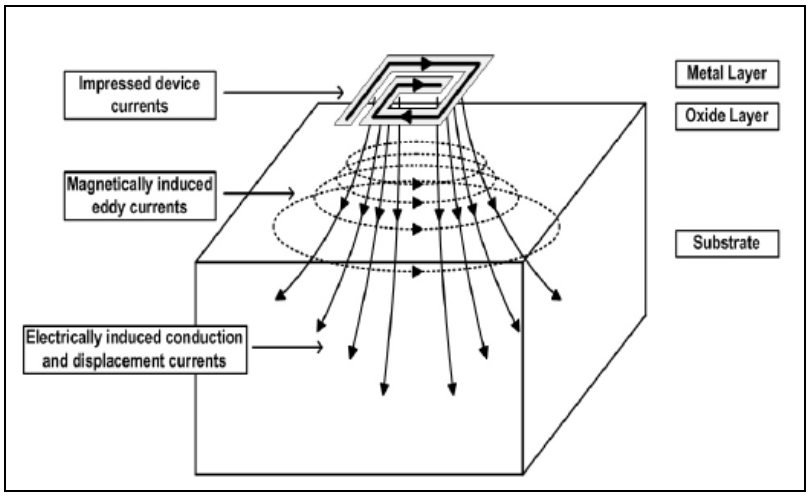

Figure 17: Eddy and displacement currents in Substrate

4.3.6 Conductance Loss

The conductor loss in an inductor is proportional to its series resistance and it increases significantly at higher frequencies due to eddy currents. Eddy currents produce non-uniform current flow in the inner portion of spiral inductors, with much higher current density on the inner side of the conductor than on the outer side.

The dc sheet resistance of a spiral coil can be reduced by using a thicker metallization but remember the lithography of the process becomes harder to control. Thick metal lines close to one another also suffer from capacitance between the two adjacent side walls.

$$R_{\mathrm{dc}} = \frac{\ell}{Wt\sigma} \quad \text{low frequencies}$$

$$R_{\mathrm{rf}} = \frac{\ell}{W\sigma\delta(1 - e^{-t/\delta})} \quad \text{high frequencies}$$

$$\text{where } \delta \text{ is the skin depth given by} \quad \delta = \sqrt{\frac{2}{\omega\mu\sigma}}$$

The depth at which the magnitude of the EM wave is decreased to 36.8% (e-1) of its intensity at the surface is called the skin depth of the metal.

4.3.7 Eddy Current Resistance

The eddy current resistance in the inductor trace is a result of current crowding that is, increasing current density along a part of the trace width. Eddy currents increase with rising frequency therefore this contribution is also frequency dependent.

- The eddy current loops produced within the trace width causes non-uniform current flow in the inner coil turns. They add to the excitation

current Icoil on the inside edge and subtract from the excitation current Icoil on the outside edge.

- Therefore, the inside edges of the coil carry current densities much larger than the outside edges, giving rise to a larger effective resistance compared to the case of uniform current flow throughout the trace width.

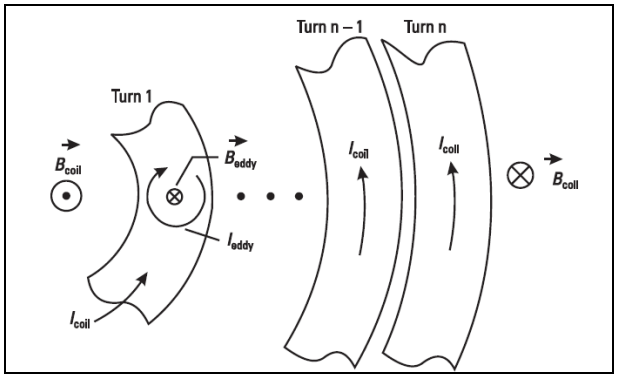

Figure 18: Eddy Fields

Because the eddy currents are induced due to time-varying magnetic fields, their values are a strong function of frequency. The critical frequency f_c at which the current crowding begins to become significant is given by the below formula where W and S are width and spacing respectively.

$$f_c = \frac{3.1(W+S)}{2\pi\mu_0 W^2} R_{sh} \qquad R_s = R_{dc}[1 + 0.1(f/f_c)^2]$$

4.4 Design Metric for On Chip Inductors

These are general set of rules which have been complied after referring to available text and simulations done on various designs along the course of the study.

- Number of Sides: If number of sides is increased maintaining external radius fixed, the perimeter increases and so does the resistance and the

inductance. But rate of increase of inductance is much faster than the rate of increase of resistance leading to increase in Quality factor. That is why circular geometry will have a higher Q compared to square geometry with same radius.

- Line spacing: At low frequencies (2 GHz or less), reduced spacing leads to increase in mutual inductance and the total inductance increases too. At higher frequencies, due to coupling between turns, larger spacing may be desirable.

- Line width: Increasing metal width will reduce the inductance (fewer turns in a given area as well as less inductance per unit length) and will decrease the series resistance of the lines at low frequencies. Large inductance area means bigger capacitance, which means lower self-resonance, and more coupling of current into the substrate. Therefore, as W goes up, inductance comes down and the frequency of Qpeak gets lower (and vice versa).
- Metal Thickness: Increasing the metal thickness (use of electroplating or using multi metal layers) increase the Q factor in the Q rising region where the frequency is below the maximum Q factor point. The resistance decreases and hence the associated losses but the inductance also slightly reduces.

- Number of Turns: More the number of turns more the inductance that can be achieved keeping the other parameters same. Increase in number of turns keeping rest geometry as same leads to an increase in area means that more current is present in the substrate, so high-frequency losses tend to be increased (capacitance to substrate and magnetically induced losses increases). Therefore, as the area goes up, inductance goes up, and the frequency of QPeak gets lower (and vice versa). The SRF also decreases due to increased inductive and capacitive coupling between traces as well as to substrate.

- Inner Diameter: Because the contribution of the innermost turn is small due to its very small inner diameter, enough empty space must be left in the center of coil to allow the magnetic flux lines to pass through it in order to increase the stored energy per unit length. With increase in inner diameter inductance increases and SRF decreases (due to increase in area). QPeak slightly increases.

- Conductivity of Substrate: Decreasing the conductivity decreases the QPeak. This does not change SRF as inductive and capacitive coupling does not change.

- Figure of Merit: For a given inductance value, one would like to have the highest possible Q and Fres in the smallest possible area of an inductor

$$\mathrm{FMI} = \frac{Q_{\mathrm{eff}} \cdot f_{\mathrm{res}}}{\mathrm{Inductor\ Area}}.$$

$$Q_{\mathrm{eff}} = \frac{\mathrm{Im}[Z_{\mathrm{in}}]}{\mathrm{Re}[Z_{\mathrm{in}}]} = \frac{X}{R}$$

$$f_{\mathrm{res}} \approx \frac{1}{2\pi\sqrt{L_{\mathrm{eff}} C_{\mathrm{eff}}}}$$

- Dielectric Layer thickness: Reduction in thickness of dielectric layer will increase the capacitive coupling and the parasitic capacitance between the substrate and spiral, consequently, the SRF of inductor is largely depressed as the thickness of dielectric layer decreases. The oxide layer can isolate the spiral and substrate, the increase of its thickness will allay the influence of substrate on the performance of inductor and reduce the parasitic capacitance. This is why the Q factors and frequency characteristics of the inductors are enhanced as the oxide layer thickness increases.
- Dielectric Layer Material: The parasitic capacitance is not only related to the thickness of dielectric layer, but also is influenced by material of dielectric layer; it increases as the permittivity of dielectric increases. The parasitic capacitances decrease when low-k material is used for dielectric layer, and the substrate losses will decline effectively to promote the performance of inductor by mitigating the capacitive coupling. The lower the permittivity of dielectric, the better the performance of inductor

4.4.1 Layout Techniques for Performance Enhancement

Tapered Design of Inductor can be considered as another option. A wide metal strip width is expected to decrease the ohmic losses. But the wide metal strip width will decrease the SRF since the increase of the inductor area. A narrow

metal strip width is expected to decrease the magnetically induced losses, especially in the center of the coil

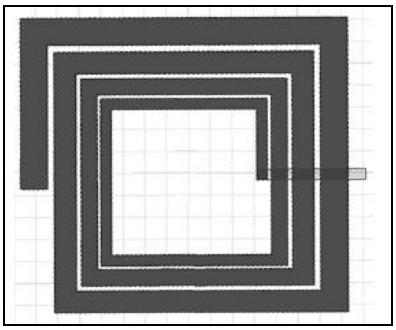

Figure 19: Tapered Design of Inductor

General Tips for Design

- The minimum metal spacing should be used to get maximum Q-factors. Upper layers of metal are typically used to implement the inductor traces because they offer lower resistance since increased metal thicknesses are allowed.
- A larger spacing gives a higher series resistance and a smaller spacing gives a high capacitive coupling and thus lower frequency of operation.
- Use of multilayers to increase the effective thickness of the spiral inductor helps reduce losses.
- Use of low loss substrates to reduce losses at high frequency.
- Thick oxide or floating inductors to isolate inductor from the lossy substrate.
- Lower permittivity and thick dielectric helps reduce the capacitance.
- Inductor turns close to the center have a negative effect on the quality of the inductor. Therefore a large hole should be made in the center of the inductor

- The geometrical optimization will help improve the performance of the inductor.

4.4.2 Quality Factor of Planar Inductor

The most fundamental definition of Q factor is given by

$$Q = 2\pi \frac{|PeakMagneticEnergy - PeakElectricEnergy|}{ElectricLossinOneOscillationCycle}$$

For an inductor, only the energy stored in the magnetic field is of interest. Any energy stored in electric field eventually is lost due to parasitic. So we can say that Q is proportional to the net magnetic energy stored.

Accurately estimating this is difficult. This is due to problems with representing parasitic as well as inductive element(s) in the model, and extracting their values from measurements.

The other definition is given by

$$Q_{CONV} = -\left[\frac{\mathrm{Im}(y_{11})}{\mathrm{Re}(y_{11})}\right] = \frac{2\omega\left(|\overline{W}_m| - |\overline{W}_e|\right)}{P_{diss}}$$

For silicon integrated inductors with typically large shunt capacitance to the substrate, thus significant electrical energy storage, QCONV can deviate from Q by a large amount. Note that Q factors extracted using above definition becomes zero near the self-resonant frequency. This result, of course, is physically unreasonable. The quality factor should not be zero at the self-resonant frequency.

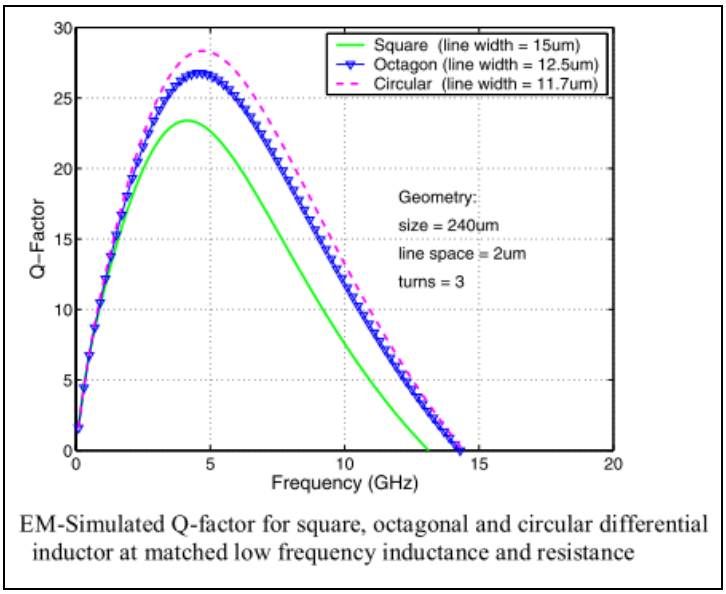

EM-Simulated Q-factor for square, octagonal and circular differential inductor at matched low frequency inductance and resistance

Figure 20: Q Factor for Standard Geometries

4.4.3 Self Resonant Frequency

Self-resonant frequency of an inductor occurs near a frequency where the difference between the average stored magnetic and electrical energy is zero, or where the imaginary part of is equal to zero.

- At low frequencies, the inductance of an integrated inductor is relatively constant. However, as the frequency increases, the impedance of the parasitic capacitance elements starts to become significant.
- SRF is the frequency at which admittance of the parasitic elements will cancel that of the inductor and the inductor will self-resonate.
- Beyond the self-resonant frequency, the parasitic capacitance will dominate and the inductor will look capacitive.
- Since parasitic capacitance increases in proportion to the size of the inductor, the self-resonant frequency decreases as the size of the inductor increases.

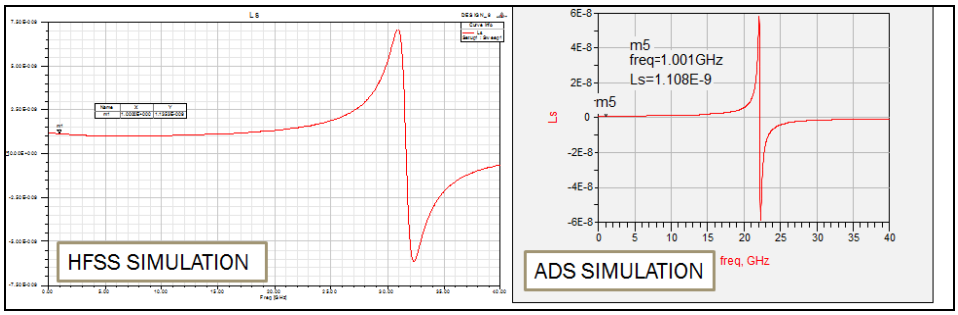

Figure 21: Simulations showing Self Resonant Frequency

4.4.4 Quality Factor Improvement Techniques

Losses associated with CMOS are generally classified into two: metal losses and substrate losses. Metal losses limit the realizable quality factor of inductors at lower frequencies while substrate losses limit thr quality factor at higher frequencies. Q-enhancement techniques are used to improve inductor Q by minimizing inductor losses

As we discussed that substrate loss at high frequencies & noise coupling can degrade quality factor. One way to alleviate this problem is to insert a ground shield to block inductor electric & magnetic field from entering the silicon. (Substrate currents are shunted ground). The problem with this approach is that the image current induced in solid ground shield (opposite direction) induces negative mutual coupling reducing the magnetic field and hence the degradation in inductance and Q factor.

A popular solution to this problem is to use a patterned ground shield (PGS) as shown below

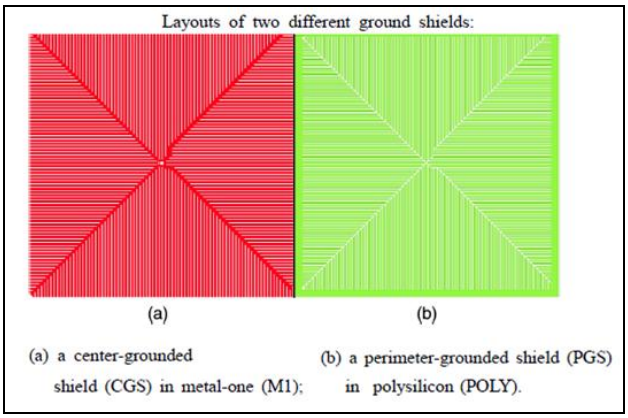

Figure 22: Patterned Ground Shield

Drawbacks of PGS

- Significant drawback to the use of a ground shield is the decrease in self-resonant frequency, which results from the increase in shunt capacitance between the coil and the ground shield plane.
- As the magnetic field passes through the patterned ground shield, its intensity is weakened due to the skin effect. This directly causes a decrease in the inductance since the magnetic flux is lessened in the space occupied by the ground shield layer. To avoid this attenuation, the shield must be significantly thinner than the skin depth at the frequency of interest.
- Knowledge of initial Rsi and Cox is required to predict the subsequent effectiveness of a PGS.

Patterned slots on the PGS cut off the path of induced image current, hence reducing disturbance of inductor magnetic field. Parameters to be considered are Geometric parameters (widths of ground strips and slots, separation between

spiral and ground shield, and lengths of strip) & Material parameter (electric conductivity of the substrate)

Ê of inductor in substrate direction is blocked by a ground shield and dissipation loss is reduced. Magnetic field disturbance is small because eddy current on ground shield is suppressed by patterned slots.

Since the quality factor is directly proportional to the series inductance. We can increase the inductance per unit area by using stacked inductors with use of different metal layers available. But these structures have increased substrate capacitance and line to line coupling capacitance.

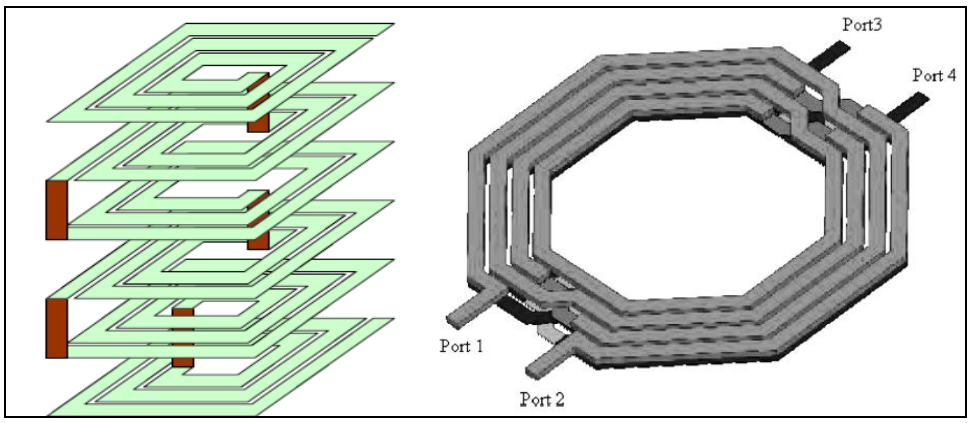

Figure 23: Stacked Inductors

CHAPTER 5

PROPOSED INDUCTOR DESIGN, MODELLING & TEST

5.1 HFSS Designs for Planar Inductors

In this chapter we will discuss square and octagonal spiral inductors made in HFSS.

5.1.1 HFSS Design of a Square Planar Inductor

Various designs were made in HFSS and their 3D models were simulated. We will discuss a few models.

The below diagram shows the theoretical model of a 3 Turns Spiral square inductor that was simulated in HFSS.

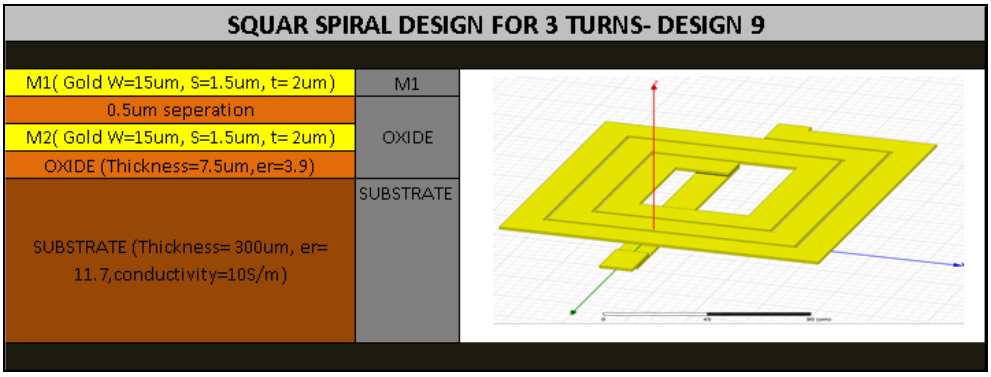

The physical dimensions of the inductor are as follows:

PARAMETER	VALUE
WIDTH (um)	15
SPACING (um)	1.5
METAL THICKNESS (um) M1	2
METAL THICKNESS (um) M2	2
Internal dia (Horizontal) (um)	50
Outer Diameter (um)	146
Number of Turns	3
Distance between M1 & M2 (um)	0.5
Thickness of oxide (um)	7.5

Table 1: Stack-up for Square Planar Inductor

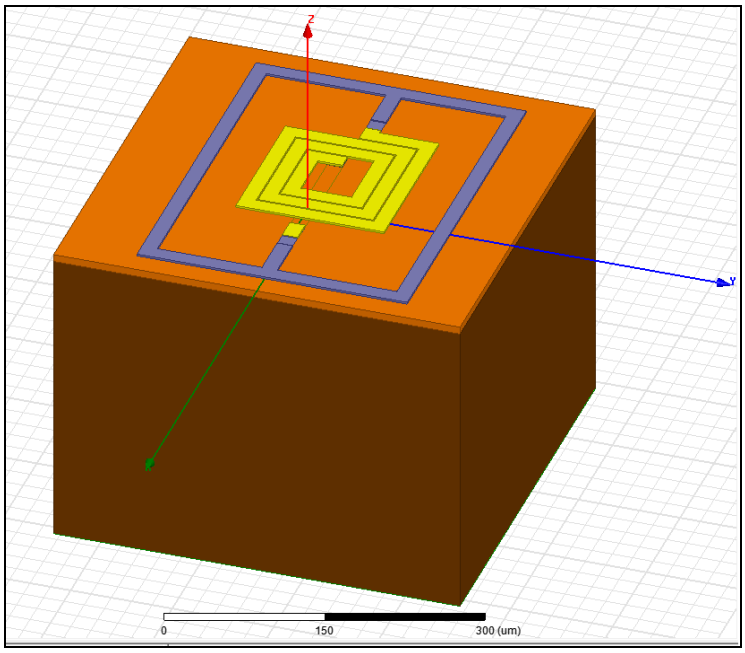

Figure 24: HFSS Model of Square Planar Spiral Inductor

The underpass is usually made of the lowest possible metal in order to decrease the inter-layer capacitance between the traces and underpass. Using a lower level of metal contributes to performance degradation and is reflected by a slight lowering of the self-resonant frequency (fsr).

5.1.2 HFSS Design of an Octagonal Planar Inductor

Octagonal inductors are preferred over square inductors due to their higher Q factor obtained at a lower inductance and resistance due to a shorter trace length. A HFSS design of octagonal inductor with internal diameter 50 um is shown below. The design is then modeled in ADS and its electrical equivalent circuit is theoretically calculated and simulated in ADS.

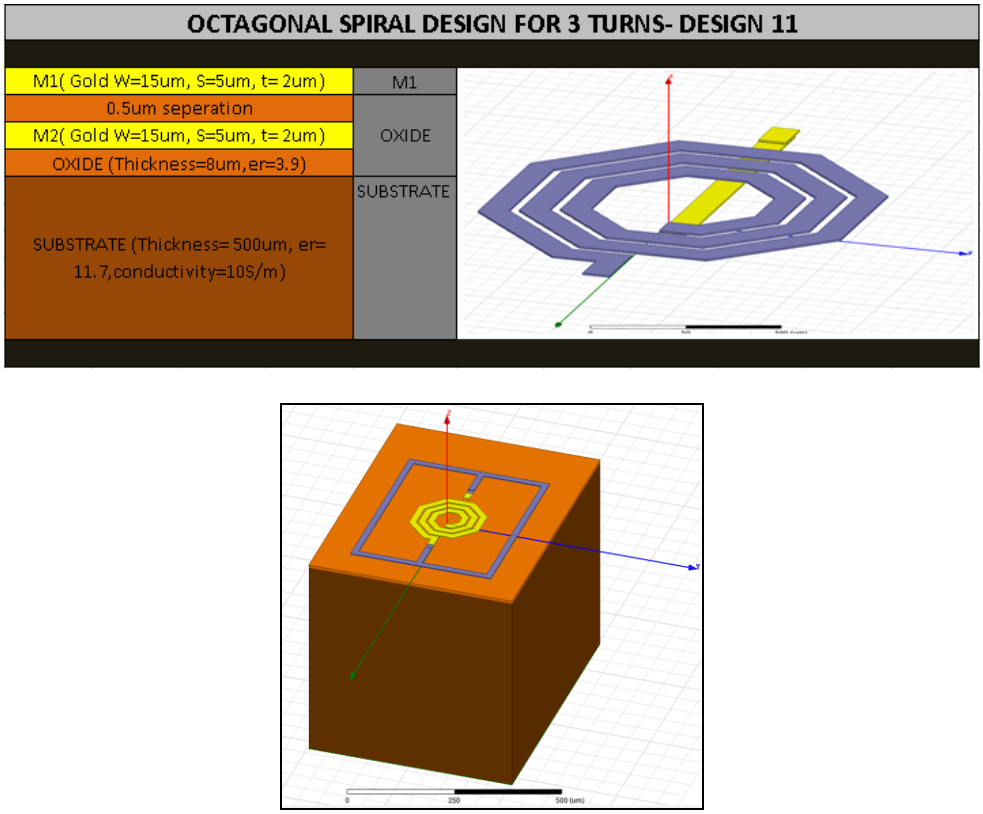

Figure 25: Octagonal Inductor in HFSS

The physical dimensions of the inductor are as follows:

INPUTS	REMARK	VALUE
w	Width of winding in um	15.000
l	Total length of inductor in um using Area	1109.842
A	Area of Inductor(in um^2)	16647.624
Dout	Outer Diameter in um	180.000
Din	Inner Diameter in um	50.000
S	Spacing between turns in um	5.000
t	Physical Thickness of top metal in um	2.000
Dm2s	Distance between top metal & substrate (um) or Thickness of Oxide	8.000
Dm2m (toxM1-M2)	Distance between metal layers in um	0.500
N	Number of turns	3.000

Table 2: Stack-up for Octagonal Inductor

5.2 Electrical Modeling of Spiral Inductors

Three models are discussed in this section which will be later used to compare with the results of HFSS simulation against the ADS simulation.

- Rsi Parasitic resistance of Substrate in ohms
- Csi Parasitic capacitance of Substrate (pF)
- Cox Capacitance between conductor and substrate in pF
- Cs Underpass to inductor track capacitance in fF
- Ls Series Inductance in nH
- Rs Series Resistance in ohms without skin effect in ohms
- Rp,Cp Represents combined effect of Csi,Cox and Rsi
- Rsub Resistance of the substrate below the inductor

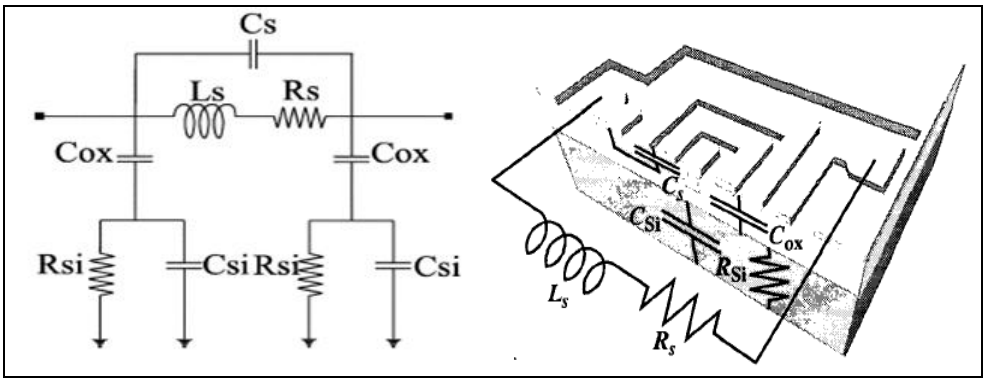

Figure 26: Model 1: Standard “pi” Model

$$Q = \frac{\omega L_s}{R_s} \cdot \frac{R_p}{R_p + \left[(\omega L_s / R_s)^2 + 1\right] R_s} \cdot \left[1 - \frac{R_s^2 (C_s + C_p)}{L_s} - \omega^2 L_s (C_s + C_p)\right]$$

$$= \frac{\omega L_s}{R_s} \cdot Substrate\ Loss\ Factor \cdot Self\ Resonance\ Factor$$

$$R_S = \frac{\rho \cdot l_T}{w \cdot t_{eff}} \qquad t_{eff} = \delta \cdot \left(1 - e^{-t/\delta}\right) \qquad \delta = \sqrt{\frac{\rho}{\pi \mu f}}$$

$$R_{Si} = \frac{2}{l \cdot \mathrm{w} \cdot G_{sub}} \qquad C_S = n \cdot \mathrm{w}^2 \cdot \frac{\varepsilon_{ox}}{t_{oxM1-M2}}$$

$$C_{ox} = \frac{1}{2} \cdot l_T \cdot \mathrm{w} \cdot \frac{\varepsilon_{ox}}{t_{ox}} \qquad C_{Si} = \frac{1}{2} \cdot l_T \cdot \mathrm{w} \cdot C_{sub}$$

Figure 27: Formulae for “pi” Model

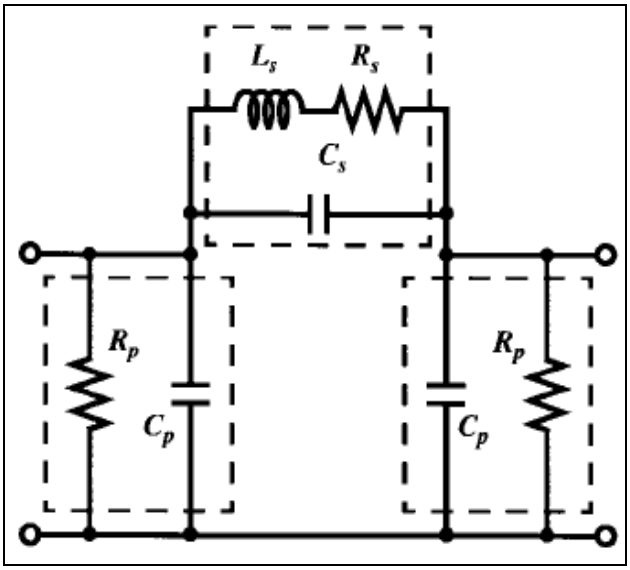

Figure 28: Model 2: Modified “pi” Model

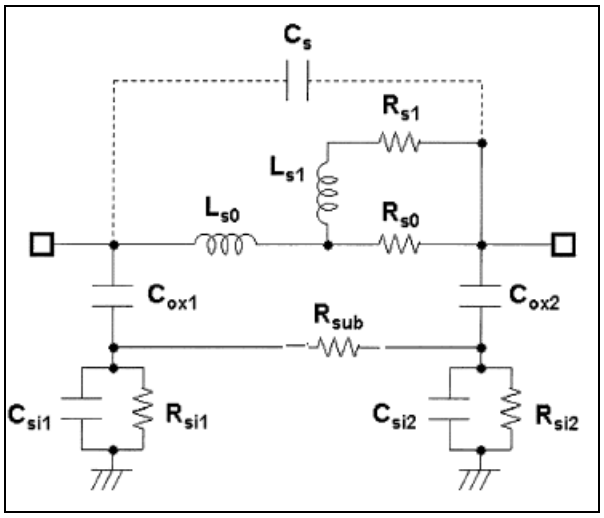

Figure 29: Model 3: Considering Parasitic and Mutual Coupling Effects

A custom made excel tool was used to calculate the parameters based on standard formulae. The excel tools also helped during the design of the inductor by predicting the co-ordinates of the geometry and hence helped to reduce the design time.

5.2.1 ADS Modelling of a Square Planar Inductors

Successful design and simulation of RFICs relies on accurate model of spiral inductors. Various model and modeling methodology of on-chip spiral inductors on silicon substrate have been reported in literature to date. We discuss some basic models and then compare the results with HFSS simulations

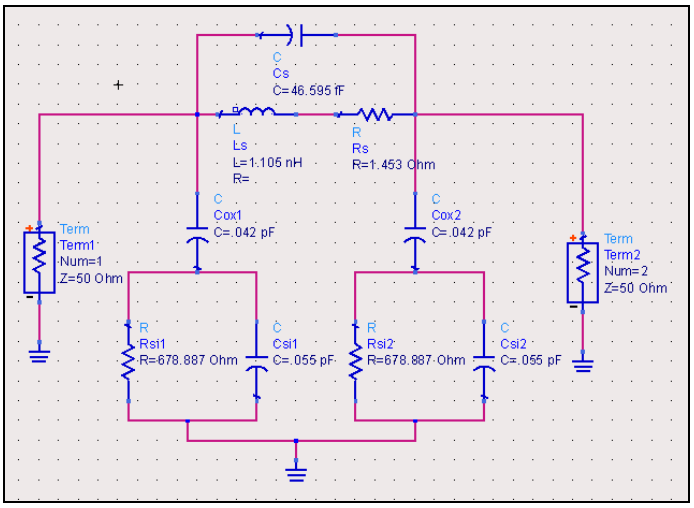

Figure 30: ADS Schematic for Model-1

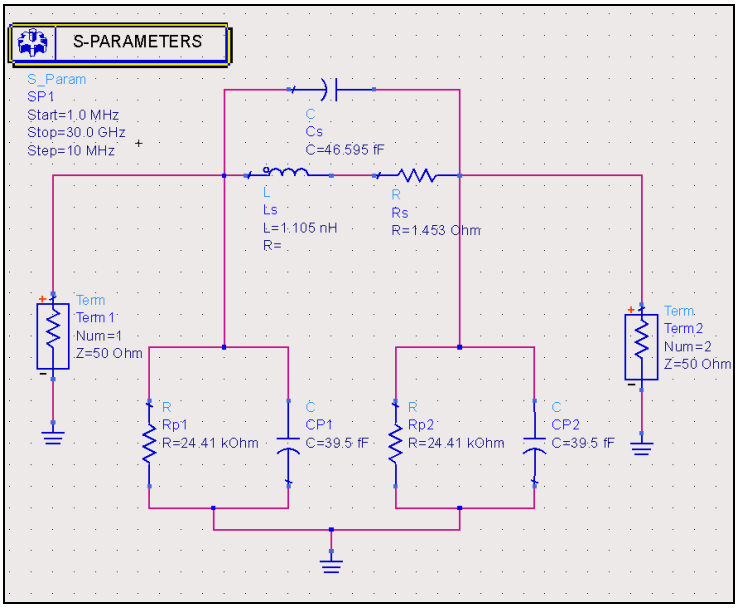

Figure 31: ADS Schematic for Model-2

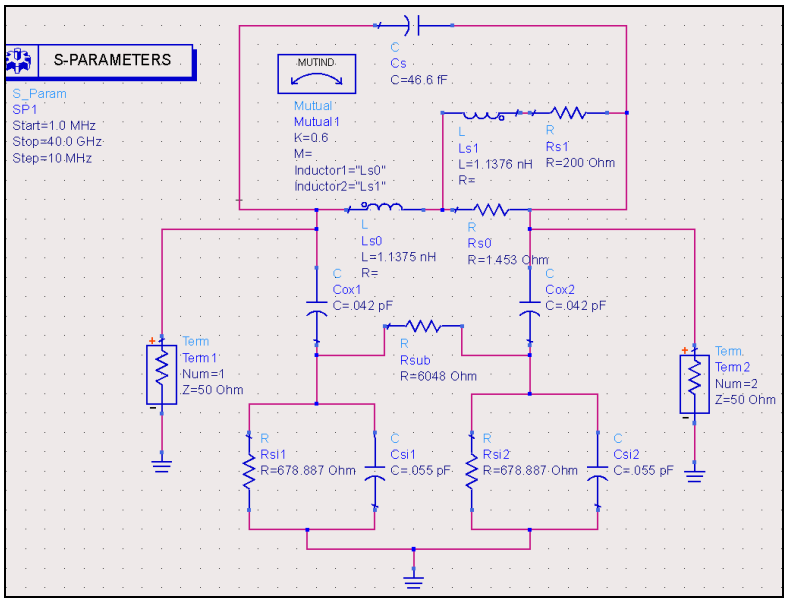

Figure 32: ADS Schematic for Model-3

5.2.2 HFSS vs ADS Results for Square Inductor

HFSS Simulation results are compared with ADS simulations results for a Square Spiral Inductor.

DESIGN-9 Freq=1GHz					
PARAMETER	EXCEL BASED CALCULATOR	HFSS	ADS (MODEL-1)	ADS (MODEL-2)	ADS (MODEL-3)
Qideal	6.948	4.63	4.758	4.758	4.604
Qprac	6.911				
Ls	1.105nH	1.135nH	1.108nH	1.108nH	1.130nH
Rs	1.453Ω	1.53Ω	1.459Ω	1.459Ω	1.538Ω
Cs	46.595fF	46.83fF	40.41fF	40.59fF	40.41fF
Rsi	678.887Ω	Not Evaluated by ADS and HFSS			
Csi	.055pF				
Cox	.042pF				
Rp	24.41KΩ				
Cp	.039pF				

Table 3: HFSS & ADS Results for Square Planar Inductor

5.2.3 HFSS vs ADS Results for Octagonal Inductor

HFSS Simulation results are compared with ADS simulations results for a Octagonal Spiral Inductor

DESIGN-11/ Freq=1GHz					
PARAMETER	EXCEL BASED CALCULATOR	HFSS	ADS (MODEL-1)	ADS (MODEL-2)	ADS (MODEL-3)
Qideal	6.768	5.55	4.638	4.638	5.412
Ls	0.973nH	1.225nH	.975nH	.975nH	1.223nH
Rs	1.314Ω	1.38Ω	1.319Ω	1.319Ω	1.416
Cs	46.595fF	48.0fF	34.70fF	34.51fF	34.7fF
Rsi	750.858Ω	Not Evaluated by ADS and HFSS			
Csi	.050pF				
Cox	.036pF				

Table 4: HFSS & ADS Results for Octagonal Planar Inductor

5.3 Symmetric Spiral Inductors

Symmetric spiral inductors are used for differential circuit applications for their robustness and superior noise rejection properties. They have higher Q compared to their non-symmetrical counterparts for the following reasons

- Presence of shorter underpass metal line and smaller number of overlaps which decreases the capacitance and consequently improves the quality factor of the inductor.
- They occupy lesser chip area compared to its asymmetrical counterpart.

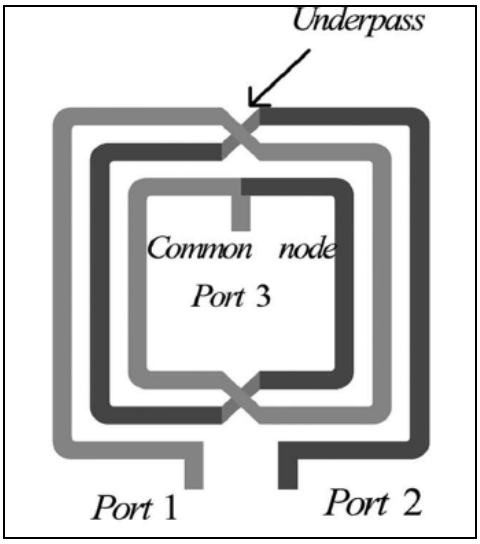

Figure 33: Symmetric Square Differential Inductor

5.3.1 Octagonal Symmetric Spiral Inductor Design

The below figure shows the HFSS model of a 4 Turn octagonal inductor symmetrical with respect to Port1 and Port2.

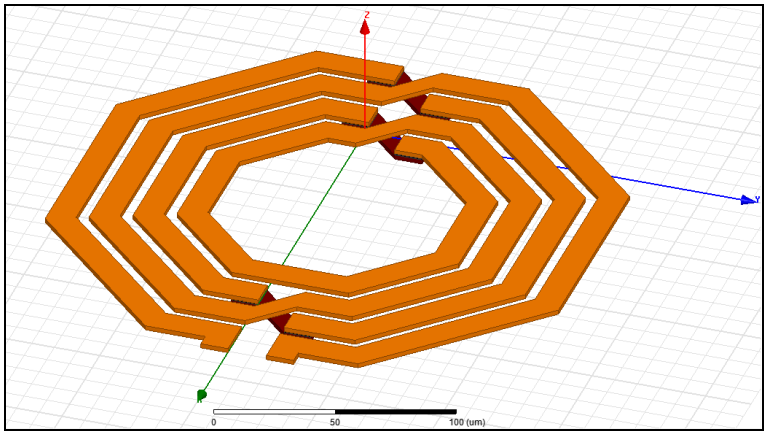

Figure 34: Symmetric Octagonal HFSS Inductor Design

PARAMETER	VALUE
WIDTH (um)	12
SPACING (um)	5
TOP METAL THICKNESS (um)	2
Internal dia (Vertical) (um)	100
Outer Diameter (Horizontal) (um)	226
Number of Turns	4
Distance between M6 & M5 (um)	0.5
BOTTOM METAL THICKNESS (um)	2
SU-8-300 THICKNESS (um) (Being used instead of SiO2)	10
Substrate THICKNESS (um)	300
SU-8-300 COATINGTHICKNESS (um) (8 um above TOP METAL layer)	10

Table 5: Stack-up for Symmetric Octagonal Inductor

SU-8 is a commonly used epoxy-based negative photo resist. It is a very viscous polymer that can be spun or spread over a thickness ranging from 0.1 micrometer up to 2 millimeters. Its maximum absorption is for ultraviolet light with a wavelength of 365 nm. When exposed, SU-8's long molecular chains cross-link causing the solidification of the material. It is also one of the most bio-compatible materials known and is often used in bio-MEMS. The SU-8 photo epoxy is used as passivation layer for measurement electrodes in the bottom part of a cell culture chamber.Adhesion of SU-8 is usually good, but depends on the material. The adhesion is worst with gold (Au), average with silicon with native oxide, and best with silicon nitride (SiN).SU-8 2000 is an improved formulation of SU-8. It claims a better adhesion on most materials, due to the change of solvent.SU-8

3000 is an improved formulation of SU-8 and SU-8 2000. SU-8 3000 allows has been formulated for improved adhesion and reduced coating stress.

The following properties for Su-8 3000 material were entered after referring to datasheets.

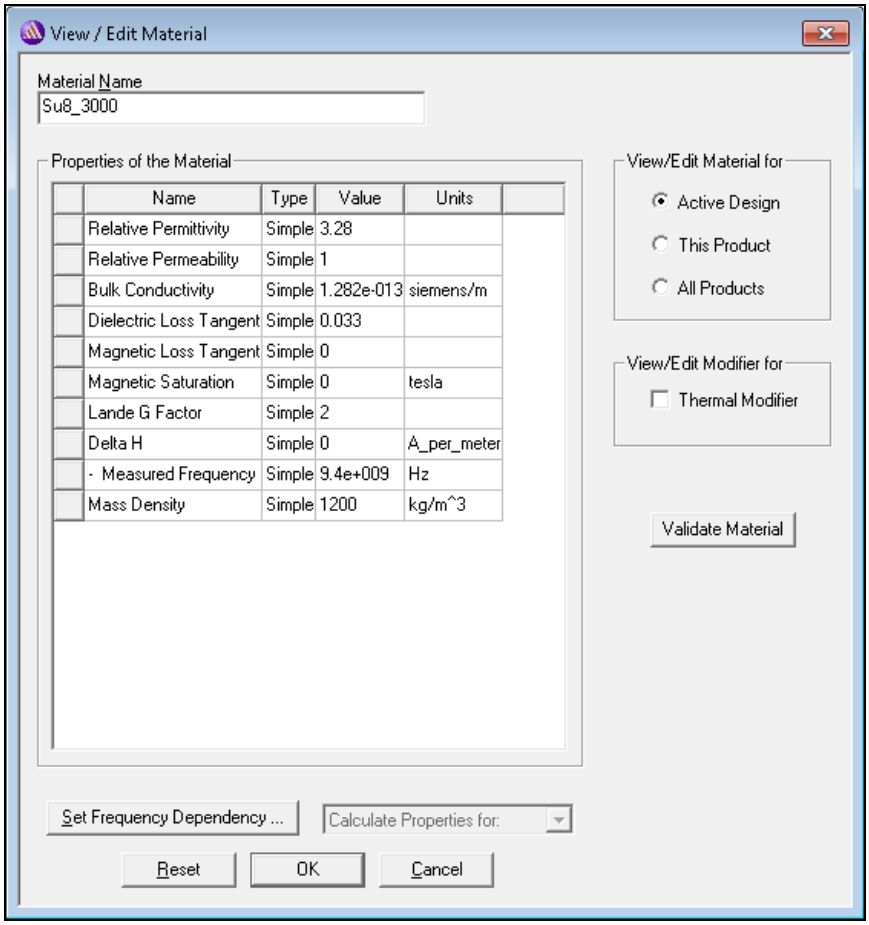

Figure 35: Properties for Su-8 3000 material

The following equations have been used in HFSS:

- Zse- Single Ended Input Impedance-> 1/Y(P1,P1)
- Zdiff- Differential Input Impedance-> 2/(Y(P1,P1)-Y(P2,P1))
- Qse- Single Ended Quality Factor-> im(Zse)/re(Zse)

- Qdiff- Differential Mode Quality Factor-> im(Zdiff)/re(Zdiff)
- Lse- Single Ended Mode inductance-> im(Zseries)/2*pi*Freq
- Ldiff- Differential Mode Inductance-> im(Zdiff)/(2*pi*Freq)

Fse (GHz)	Qse	Lse (nH)	Rs(se) (Ω)	Cs(se) (fF)	Fdiff (GHz)	Qdiff	Ldiff (nH)	Rs(diff) (Ω)	Cs(diff) (fF)
3.65	**12.97**	**2.98**	**3.61**	**45.57**	**5.20**	**15.96**	**2.88**	**3.84**	**43.56**

Table 6 Simulation Summary for Symmetric Octagonal Inductor (SU-8)

The below result was taken with the same geometry but SiO2 was used as dielectric and SU-8-3000 coating was not used. This is just for reference.

Fse (GHz)	Qse	Lse (nH)	Rs(se) (Ω)	Cs(se) (fF)	Fdiff (GHz)	Qdiff	Ldiff (nH)	Rs(diff) (Ω)	Cs(diff) (fF)
3.87	**12.94**	**2.78**	**3.36**	**50.27**	**6.51**	**17.91**	**3.03**	**2.13**	**45.75**

Table 7: Simulation Summary for Symmetric Octagonal Inductor (SiO2)

HFSS Simulation Results

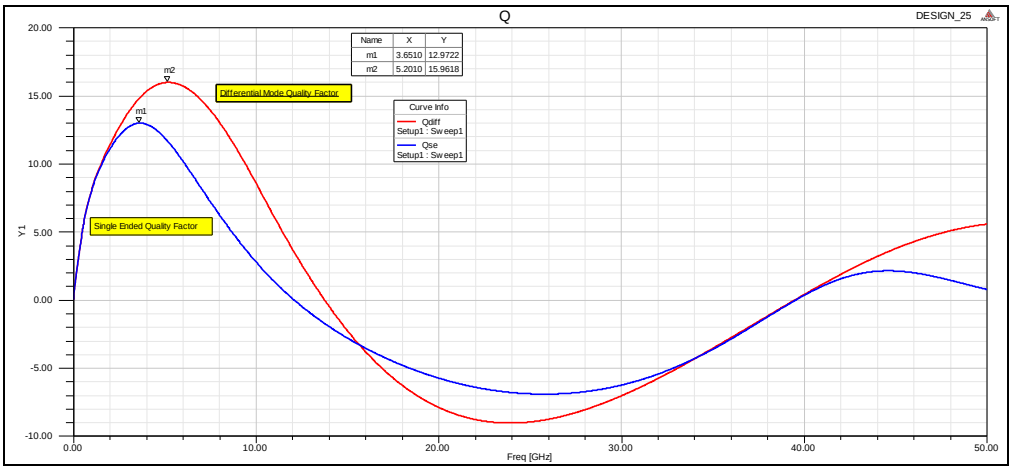

Figure 36: Plot of Quality Factor

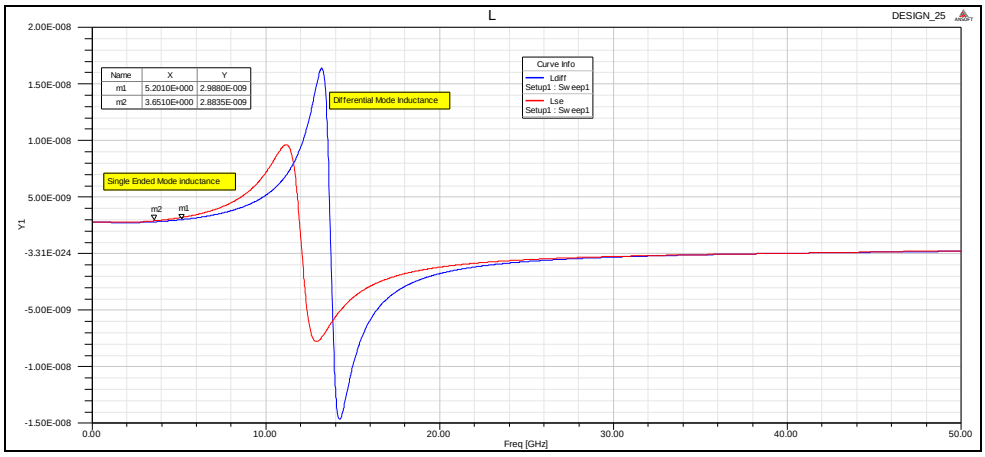

Figure 37: Plot of Inductance

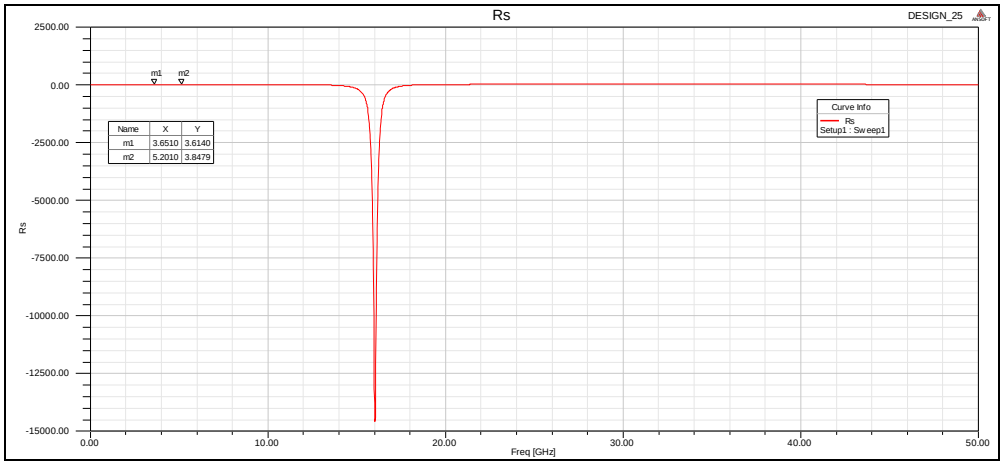

Figure 38: Plot of Series Resistance

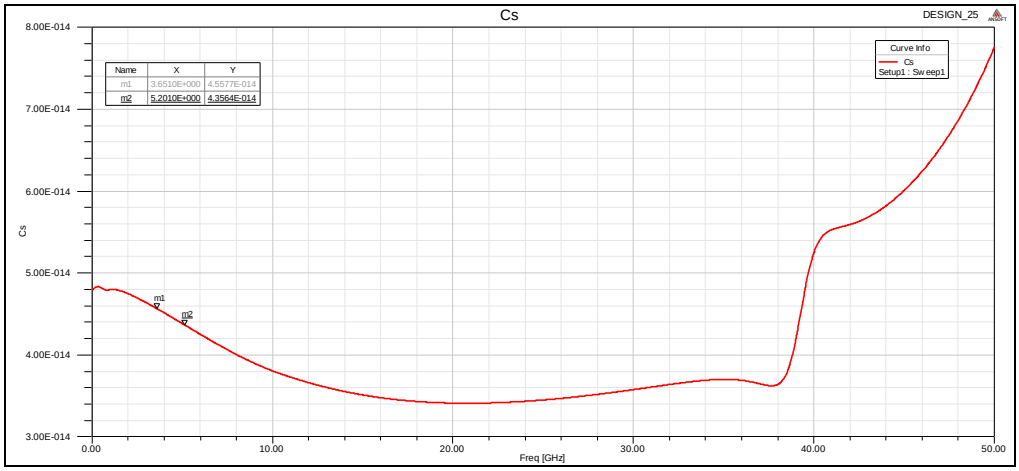

Figure 39: Plot of Capacitance

5.4 Test & Characterization of On-Chip Inductors

In order to probe a circuit we need to launch a signal into it with some type of transmission line, usually 50 ohms. This requires at least two conductors, the "signal" conductor and the "ground" conductor.

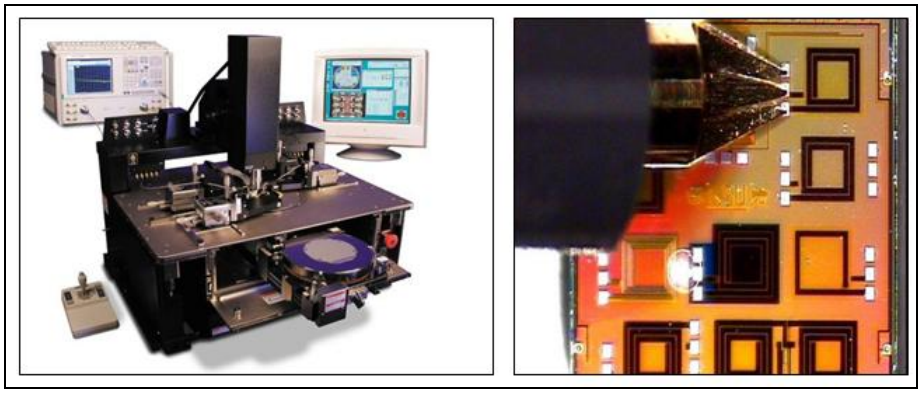

Figure 40: Test & Characterization of Spiral Inductor

Probe pitch is the distance between center-to-center of the probe tips. Typical values are 150, 250 microns. The larger probe pitch is not practical for millimeter-wave frequencies. For network analyzer calibration standards like OPEN, SHORT, LOAD & THRU would be used. Ground-signal-ground is the most common type of RF probe. This is similar to coplanar waveguide.

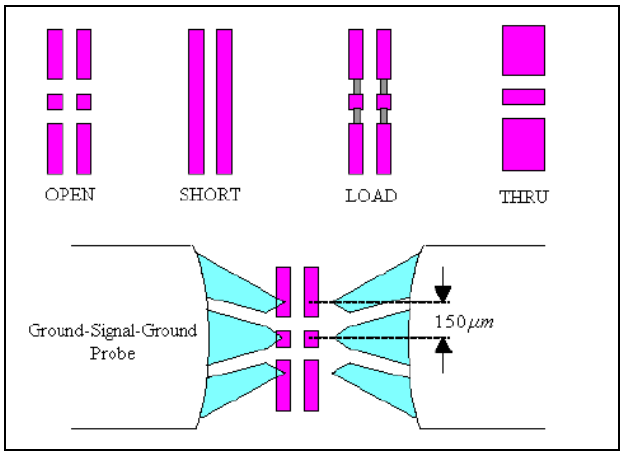

Figure 41: Calibration Substrate Probing

CHAPTER 6

CONCLUSION

The dynamic growth in wireless and RF portable electronics has driven the need of high performance on chip passive components. The study addressed this topic and was focused on planar spiral inductor design on silicon. We discussed the physical and electrical model along with design techniques to optimize its performance. Different design and simulations were presented and then compared to get a better understanding.

A RF-Bio sensing design proposal was also made for applications like drug testing and discovery which is based on a through hole spiral symmetric octagonal design simulated in HFSS.

To conclude this work will be useful for the researchers interested in design and development of RFICs involving on chip inductors.

REFERENCES

[1] Hua Wang; Sideris, C.; Hajimiri, A.; , "A frequency-shift based CMOS magnetic biosensor with spatially uniform sensor transducer gain," Custom Integrated Circuits Conference (CICC), 2010 IEEE , vol., no., pp.1-4, 19-22 Sept. 2010

[2] Hua Wang; Yan Chen; Hassibi, A.; Scherer, A.; Hajimiri, A.; , "A frequency-shift CMOS magnetic biosensor array with single-bead sensitivity and no external magnet," Solid-State Circuits Conference - Digest of Technical Papers, 2009. ISSCC 2009. IEEE International , vol., no., pp.438-439,439a, 8-12 Feb. 2009

[3] Telli, A.; Demir, I.E.; Askar, M.; , "Practical performance of planar spiral inductors," Electronics, Circuits and Systems, 2004. ICECS 2004. Proceedings of the 2004 11th IEEE International Conference on , vol., no., pp. 487- 490, 13-15 Dec. 2004

[4] C.C.; Yeo, K.S.; Chew, K.W.; Tan, C.Y.; Do, M.A.; Ma, J.G.; Chan, L.; , "Equivalent circuit model of a stacked inductor for high-Q on-chip RF applications," Circuits, Devices and Systems, IEE Proceedings - , vol.153, no.6, pp.525-532, Dec. 2006

[5] Abu-Nimeh, F.T.; Salem, F.M.; , "Integrated magnetic array for bio-object sensing and manipulation," Biomedical Circuits and Systems Conference (BioCAS), 2010 IEEE , vol., no., pp.62-65, 3-5

[6] Hua Wang; Sideris, C.; Hajimiri, A.; , "A frequency-shift based CMOS magnetic biosensor with spatially uniform sensor transducer gain," Custom Integrated Circuits Conference (CICC), 2010 IEEE

[7] Ji Chen; Liou, J.J.; , "Improved and physics-based model for symmetrical spiral inductors," Electron Devices, IEEE Transactions on , vol.53, no.6, pp. 1300- 1309, June 2006

[8] Reiha, M.T.; Tae-Young Choi; Jong-Hyeok Jeon; Mohammadi, S.; Katehi, L.P.B.; , "High-Q differential inductors for RFIC design," Microwave Conference, 2003. 33rd European , vol.1, no., pp. 127- 130 Vol.1, 7-9 Oct. 2003

[9] Murphy, O.H.; McCarthy, K.G.; Delabie, C.J.P.; Murphy, A.C.; Murphy, P.J.; , "Design of multiple-metal stacked inductors incorporating an extended physical model," Microwave Theory and Techniques, IEEE Transactions on , vol.53, no.6, pp. 2063- 2072, June 2005

[10] Yu Cao; Groves, R.A.; Xuejue Huang; Zamdmer, N.D.; Plouchart, J.-O.; Wachnik, R.A.; Tsu-Jae King; Chenming Hu; , "Frequency-independent

equivalent-circuit model for on-chip spiral inductors," Solid-State Circuits, IEEE Journal of , vol.38, no.3, pp. 419- 426, Mar 2003

[11] Yue, C.P.; Ryu, C.; Lau, J.; Lee, T.H.; Wong, S.S.; , "A physical model for planar spiral inductors on silicon," Electron Devices Meeting, 1996. IEDM '96., International , vol., no., pp.155-158, 8-11 Dec. 1996

[12] Mohan, S.S.; del Mar Hershenson, M.; Boyd, S.P.; Lee, T.H.; , "Simple accurate expressions for planar spiral inductances," Solid-State Circuits, IEEE Journal of , vol.34, no.10, pp.1419-1424, Oct 1999

[13] On-Chip Spiral Inductors for RF Applications:An Overview by Ji Chen and Juin J. Liou

[14] Hizon, J.R.E.; Rosales, M.D.; Alarcon, L.P.; Sabido, D.J.; , "Integrating spiral inductors on 0.25 μm epitaxial CMOS process," Microwave Conference Proceedings, 2005. APMC 2005. Asia-Pacific Conference Proceedings , vol.1, no., pp. 4 pp., 4-7 Dec. 2005

[15] Ban-Leong Ooi; Dao-Xian Xu; Pang-Shyan Kooi; , "A comprehensive explanation on the high quality characteristics of symmetrical octagonal spiral inductor," Radio Frequency Integrated Circuits (RFIC) Symposium, 2003 IEEE , vol., no., pp. 259- 262, 8-10 June 2003

[16] Burghartz, J.N.; Edelstein, D.C.; Soyuer, M.; Ainspan, H.A.; Jenkins, K.A.;, "RF circuit design aspects of spiral inductors on silicon," Solid-State Circuits, IEEE Journal of , vol.33, no.12, pp.2028-2034, Dec 1998

[17] F. W. Grover, Inductance Calculations, Van Nostrand, Princeton, N.J., 1946; reprinted bv Dover Publications. New York, N.Y., 1962.

[18] Biosensors:A tutorial review Sarja Mohanty & Elias KOUGIANOS

[19] Review Paper Electrochemical Biosensors - Sensor Principles and Architectures Dorothee Grieshaber, Robert MacKenzie, Janos and Erik Reim